Ion distributions of different Kronian plasma regions

Zoltán Németh,[1] Karoly Szego,[1] Zsófia Bebesi,[2] Géza Erdős,[1] Lajos Foldy,[1] Abigail Rymer,[3] Edward C. Sittler,[4] Andrew J. Coates,[5] and Anne Wellbrock[5]

Received 18 February 2011; revised 18 May 2011; accepted 7 June 2011; published 13 September 2011.

[1] Plasma data from the Cassini Plasma Spectrometer experiment were used to investigate the properties of the variable plasma environment of Titan's orbit. The characteristics of this plasma environment play a crucial role in the plasma-moon interaction and also have a strong influence on the ionosphere of Titan. Using dynamic energy spectra of ions within ±3 h of the Titan flybys we identified different ambient plasma environments, similar to the ones proposed earlier based on electron measurements. Expanding the time interval to 12 h to cover full SKR periods, and taking into account the composition of the ions, we showed that the longer intervals include all the previous categories, and a special one, a short event, rich in heavy ions. Detailed study of the vicinity of these events revealed the fine structure of the magnetodisk of Saturn, having a narrow central sheet of very high heavy ion content, heavy rich events occurring when the spacecraft crosses this central sheet. We also proved that the heavy rich events appear periodically in longitude, but with a period slightly (by 0.35°/day) longer than the SLS3 period.

Citation: Németh, Z., K. Szego, Z. Bebesi, G. Erdős, L. Foldy, A. Rymer, E. C. Sittler, A. J. Coates, and A. Wellbrock (2011), Ion distributions of different Kronian plasma regions, *J. Geophys. Res.*, *116*, A09212, doi:10.1029/2011JA016585.

1. Introduction

[2] The plasma environment of Titan is highly variable; the Cassini spacecraft has found strongly altered plasma properties for each encounter, even if the consecutive flybys take place at similar Saturn Local Time (SLT). The properties of the plasma are influenced by the solar radiation, the solar wind, and rotating plasma and magnetic structures [*Burch et al.*, 2009; *Arridge et al.*, 2008]. The characteristics of this plasma environment play a crucial role in the plasma-moon interaction and also have a strong influence on the ionosphere of Titan.

[3] Titan has an extended atmosphere composed mostly of nitrogen, a few percent of methane and a fraction of complex organic material [*Niemann et al.*, 2005]. Since Titan has no intrinsic magnetic field, and is orbiting Saturn within its magnetosphere, the high energy charged particles can directly bombard the upper atmosphere. The ionosphere of Titan is formed by three dominant processes [*Gurnett et al.*, 1982; *Galand et al.*, 2006]: photoionization by solar EUV radiation, electron impact ionization and charge transfer of flowing plasma with neutrals. The interaction between Saturn's magnetic field and the extended atmosphere of Titan creates an induced magnetosphere [*Ness et al.*, 1982; *Backes et al.*, 2005].

[4] The constantly changing solar wind dynamic pressure accounts for the variability of the volume and the boundary layers of the Kronian magnetosphere. Due to the compression of the magnetosphere the Cassini Titan encounters sometimes take place in the magnetosheath. On the other hand the internal dynamics of the magnetosphere (including several corotating and other magnetic and plasma phenomena) also alter the properties of the plasma flow near the orbit of Titan. The corotating coordinate system based on the observations of the Saturn Kilometric Radiation [*Gurnett et al.*, 2005; *Kurth et al.*, 2008] is the natural reference frame of these phenomena. The rotation period of this coordinate system is approximately 10.7 h and slightly varying. The variation is of the order of one percent on timescales of a few years [*Galopeau and Lecacheux*, 2000; *Gurnett et al.*, 2005]. Cassini observations [*Gurnett et al.*, 2009] suggest that the period is different for the northern and southern hemispheres. This double periodicity was found in the magnetic field data as well [*Southwood*, 2011]. *Burch et al.* [2009] showed that in the SKR system the heavy ions form a cam shaped structure, which extends to 25 R_S (well beyond the orbit of Titan) between 0° and 45° longitudes. Magnetic field measurements also exhibit the SKR periodicity [*Arridge et al.*, 2008; *Kellett et al.*, 2009].

[5] Due to this variability the actual encounters can eventuate in very different plasma environments. For the naming of these different regions, we will follow the ter-

[1]Department of Space Physics, KFKI Research Institute for Particle and Nuclear Physics, Budapest, Hungary.
[2]Max Planck Institute for Solar System Research, Katlenburg-Lindau, Germany.
[3]Johns Hopkins University Applied Physics Laboratory, Laurel, MD, USA.
[4]NASA Goddard Space Flight Center, Greenbelt, MD, USA.
[5]Planetary Group, Mullard Space Science Laboratories, University College London, Dorking, UK.

Copyright 2011 by the American Geophysical Union.
0148-0227/11/2011JA016585

minology of *Gombosi et al.* [2009], who give a comprehensive description of the structure of the Kronian magnetosphere. The dynamics of this structure and its interaction with Titan is the subject of several recent articles [*Burch et al.*, 2009; *Rymer et al.*, 2009; *Sittler et al.*, 2009; *Simon et al.*, 2010]. *Simon et al.* [2010] identified current-sheet and lobe-type regions based on the radial component of the magnetic field. *Rymer et al.* [2009] have given a classification of the first 50 Titan encounters based on electron measurements. In that paper the authors identified four characteristic electron signatures, and classified the encounters based on the dominant electron signatures of the upstream plasma. They defined "plasma sheet," "lobe-like," "magnetosheath" and "bimodal" type encounters as well as "mixed" (showing the properties of two or more of the above mentioned "clear" types) and a few encounters remained "unclassified."

[6] Using CAPS IMS data [*Young et al.*, 2004], we study the global features of ion distributions around Titan. Our analysis reveals a very rich ion structure, and the relationships of the different encounter types. We evaluated the relative importance of the solar and corotating effects, and found that in most cases the position of the encounter with respect to the magnetodisk and the magnetosheath determines the type of the encounter.

[7] Our first step is to identify characteristic ion signatures of the plasma around the orbit of Titan. We chose these signatures as the basis of our further investigations.

[8] Next we examined the different classes of *Rymer et al.* [2009] in view of our findings about the ion signatures. We found that each of their classes is associated with a characteristic ion plasma type, but shorter occurrences of other types are prevalent. In other words, in closer examination every encounter falls into their "mixed" category. Thus we performed a refinement of the classification examining shorter (34 min) time intervals in a wider (12 h long) window of interest around each of the first 54 encounters.

[9] Then we conducted a statistical analysis of the plasma environment types as discussed below. We related these types with the regions of the magnetosphere, so it is possible now to use the plasma data to investigate the structure and even the fine structure of magnetospheric phenomena e.g., the magnetodisk. We also studied the SKR dependence of the structure.

2. Instrumentation

[10] The Cassini Plasma Spectrometer (CAPS) consists of three independently operated plasma sensors [*Young et al.*, 2004], the Ion Mass Spectrometer (IMS) [*McComas et al.*, 1998; *Nordholt et al.*, 1998], the Ion Beam Spectrometer (IBS) [*Vilppola et al.*, 2001] and the Electron Spectrometer (ELS) [*Linder et al.*, 1998]. The IMS is designed for ion plasma dynamics and composition analysis (1 eV to 50 keV), the IBS is to detect ion velocity distributions of narrow beam-like structures in the energy range of 1 eV to 50 keV and ELS measures electron distributions in the energy range 0.5 eV to 28 keV.

[11] For our study we used the data of the IMS sensor, a top-hat electrostatic analyzer designed to measure ion energies up to ~50 keV/charge. The field of view (FOV) of IMS in the azimuthal direction is ~10°–12° wide and there are 8 elevation channels each of which have about 20° wide FOV in the perpendicular direction. The instrument is also capable of performing time-of-flight (TOF) analysis of the ions by summing data for a 256 s long period of time over all directions. In the Singles mode, which we use for this study, a full energy sweep for 63 logarithmically spaced energy channels achieved during 32 s, without mass separation.

[12] The whole CAPS package is set on a motor driven actuator, which perform a windshield-wiper-like motion with a variable length interval in the ambient plasma flow. Its rotation axis is parallel with the z axis of the spacecraft.

3. The Method

[13] Since the FOV of CAPS IMS in the azimuthal direction is limited to ~10°–12° the instrument only samples a slice of the phase space for every individual measurement. The view direction is changing due to the actuator motion and spacecraft maneuvers, so eventually the instrument samples a good part of the phase space, but for any given time we do not know the complete phase space distribution of the ions. Thus for an anisotropic distribution (that means: in most real cases) the viewing conditions play a very important role. For a beam distribution for example it is impossible to tell the flux of the flow if the viewing is inappropriate.

[14] The first question of the data analysis is whether the information we are interested in can be deduced from the measured count rates with or without any further approximations. If not, we can limit our analysis to the times of favorable viewing, or we can try to find parameters, which are less sensitive to viewing conditions but are still capable to answer our questions. Our goal was to characterize the different plasma regions of the Kronian magnetosphere around the Titan encounters. We needed a method, which makes that possible with the fullest possible time coverage.

[15] Earlier papers analyzed the ion plasma environment of Saturn based on density temperature and velocity moments [*Thomsen and Delapp*, 2005; *Wilson et al.*, 2008; *Thomsen et al.*, 2010; *Szego et al.*, 2010; *Nemeth et al.*, 2010]. Although the methods based on moments are highly effective, they require appropriate viewing. The variable measurement conditions make it very difficult, sometimes completely impossible to determine the moments. In a significant amount of time we have no moments, although we have high quality plasma measurements. Other methods also eliminate a large part of the data to overcome the influence of the variable viewing conditions, by using only data acquired with particular sensors that were viewing closely into the corotational flow direction [*Burch et al.*, 2009].

[16] By analyzing SNG data of the CAPS IMS [*Young et al.*, 2004] instrument we found that to tell apart the different regions of the magnetosphere it is not necessary to have quantitative density temperature or velocity values. Abrupt changes in the count rates, in the relative weight of the low and high energy ion components, and/or in the position and width of the peaks associated with these components appear in the time-dependent energy spectrogram (dynamic spectrum), which reliably characterize the different plasma environments, even in less favorable viewing conditions, when the moment calculation is impossible.

[17] The limited field of view (FOV) of the CAPS instrument actuating and otherwise moving with the some-

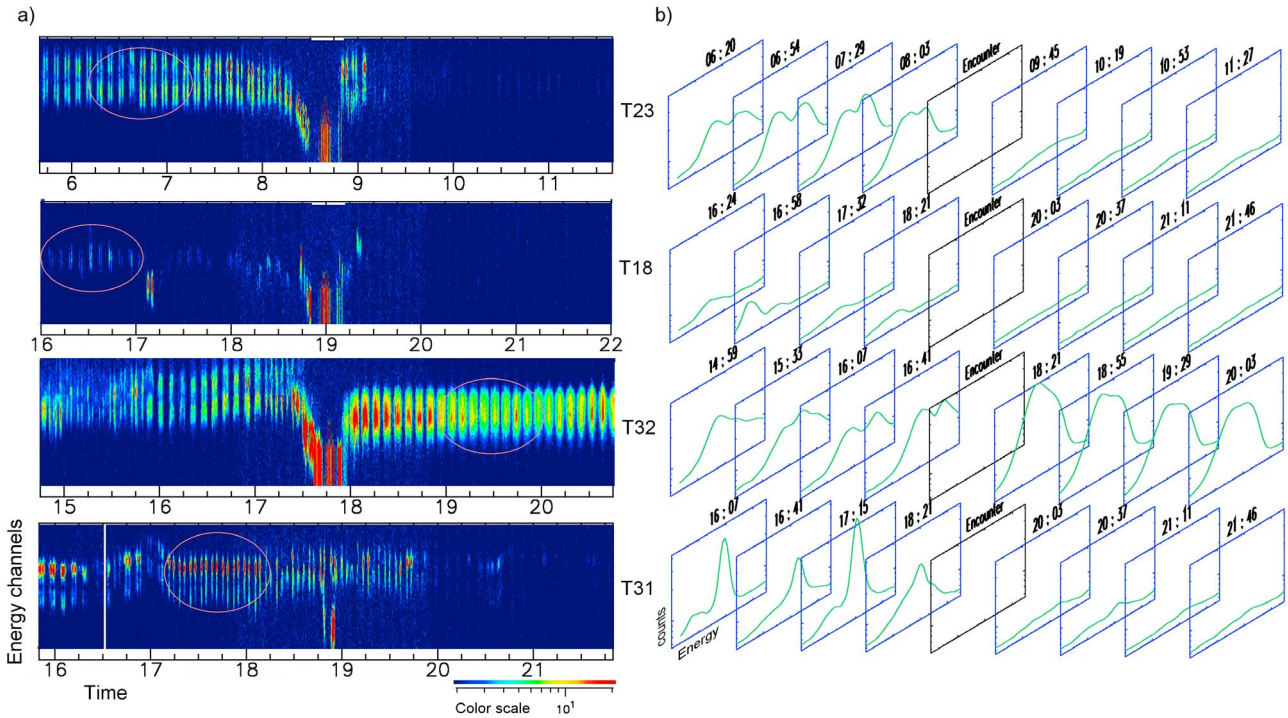

Figure 1. (a) Time-dependent energy spectrograms (dynamic spectra) of the four basic plasma types. Regions marked by a circle show data from a single basic plasma type. From top to bottom: T23, plasma sheet; T18, lobe-like; T32, magnetosheath; T31, bimodal. (b) Stacked plots of 34 min averaged energy spectra for the same time periods.

times rolling spacecraft makes it very complicated to determine the relationship of the plasma moments and the actual count rates. But we nonetheless can compare count rates coming from the same direction in consecutive actuator sweeps. If we suddenly have much more particles in the same direction and later the count rate drops to the previous level again, we can safely state that the probe crossed plasma of another type. If the flow direction changes slowly we still can compare the data of consecutive sweeps. On the other hand abrupt changes in the flow direction also indicate that the probe enters a different plasma regime. Similarly the relative flux of the lighter and heavier ions is less affected by the FOV problem. The mean energy or the actual thermal speed of an ion component can also be a good indicator of the variation of the plasma environment. All of these parameters can be extracted from the dynamic spectrum. Most of the time all of these indicators change in unison in the transition regions of the different plasma regimes, which makes this method very robust in identifying the different plasma types.

4. Classification

[18] To find the different characteristic ion signatures of the plasma we studied the ion data obtained by the IMS sensor. In the Singles mode, which we use for this study, a full energy sweep for 63 logarithmically spaced energy channels is achieved during 32 s, without mass separation. We used data measured 3 h before and after the encounters. The immediate vicinity (±30 min, i.e., 4–5 R_T from Titan) of the encounter was omitted from our analysis, since we wanted to study the plasma environment affecting the encounter and not the other way around. For better signal-to-noise ratio we summed over the eight anodes of the sensor. For our initial analysis, we plotted the spectrograms in a custom color code, specifically chosen to emphasize the relatively small differences occurring in the upstream plasma. We have checked these plots to find (and exclude) any anomalous data apparent in the spectrograms. We have also calculated and plotted longer time averaged energy spectra around the encounters.

[19] The most apparent feature of the spectrograms is the presence of two strong peaks due to the lower and higher energy ion components of the plasma. Analysis of the time of flight (TOF) spectra has showed that these peaks are associated with the lighter and heavier ion components of the plasma respectively [see, e.g., *Thomsen et al.*, 2010]. The two peaks shift back and forth along the energy axis; their intensities also show significant variations.

[20] For many encounters the count rates are very low after the encounter. This is due to the spacecraft maneuvers in connection with remote sensing operations. Still the relative intensity of the peaks (if they are visible) suggests variability similar to the upstream conditions.

[21] We found several significantly different plasma regions (types) with significantly different ion signatures; not only the ion energy and flux, but the ion composition also is different for the different types. In Figure 1 we show examples of the dynamic spectra of these types, together with stacked plots of 34 min averaged energy spectra of the same time periods.

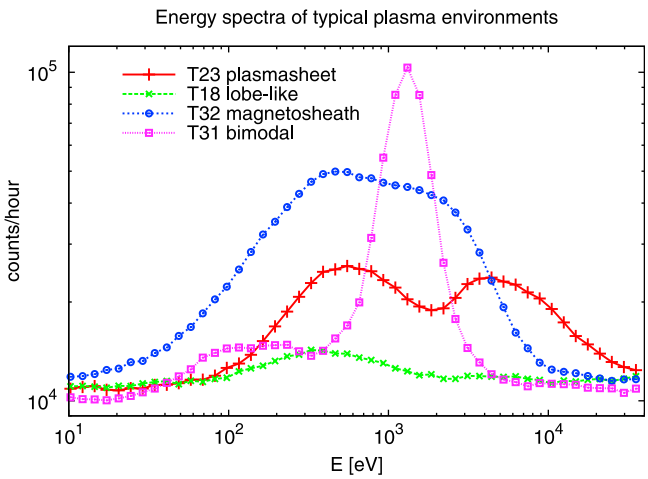

Figure 2. Energy spectra of typical plasma environments. We based our statistical studies on the pronounced differences of the four spectra. (These differences highly exceed the errors of the spectra, since the standard deviations are smaller than the markers used to represent the data points.)

[22] In the next subsections we present the ion properties of the four basic plasma environment types. For each type we list the characteristic properties and show one hour averaged energy spectra in Figure 2. The findings of these subsections will serve as the basis of our more detailed studies.

4.1. Plasma Sheet Encounters

[23] The plasma environment of this type is characterized by a clear double-peaked energy/charge ion spectrum. A lower energy peak corresponding to the proton group can be found at ~400–600 eV, and a higher energy peak corresponding to the heavier (water group) ions is at ~4400 eV. The intensities of the two peaks are similar; the instrument measured 15–20,000 counts/hour in the energy channels for both peaks. A roughly 10,000 counts/hour flat background was already subtracted to obtain these values as well as the results of the following subsections.

4.2. Lobe-like Encounters

[24] This encounter type is also characterized by a double-peaked energy/charge ion spectrum, in which the higher energy peak is highly suppressed relative to the light ion peak. The characteristic energies are pretty much the same as that of the previous type, but the intensities are much lower. A few thousand counts/hour is typical for the low energy peak and the high energy peak is even smaller. The lobe-like plasma is composed mostly of light ions. The low heavy/light ratio is perhaps the most distinctive characteristic of the lobe-like type.

4.3. Magnetosheath Encounters

[25] In this type the instrument found plasma originating from the magnetosheath of the Kronian magnetosphere as approaching Titan. The ion signature of this plasma type is a very broad and intense peak in the energy/charge spectrum between 150 eV and 35000 keV (energies of half maximum), with count rates as high as 50,000 counts/hour. The high count rates and this broad structure adequately identify the ion plasma of these regions. We found only a few cases (T32, T42) of this type.

4.4. Bimodal or Heavy-Rich Encounters

[26] This type is again characterized by a clear double-peaked energy/charge ion spectrum. The peaks are shifted toward the lower energy regime (about 250 and 1500 eV for the proton and heavy ion groups respectively) relative to the plasma sheet and lobe-like spectra. The height of the low energy peak is similar to that of the plasma sheet type, but the heavy ion peak is much higher (about 100,000 counts/hour) and much more narrow. In ion measurements, no apparent bimodality shows up for this environment type (no more than for the other types anyway); the most characteristic feature is its high content of cold heavy ions. Thus, from the point of view of the ion data, this plasma type cannot be called "bimodal," but the encounters dominated by this heavy-rich plasma coincide with that classified as bimodals based on the electron measurements.

[27] We classified (see Table 1) the encounters according to the most characteristic plasma type present in the ±3 h vicinity of the closest approach, and then compared our results to the electron classification of *Rymer et al.* [2009]. After careful examination of the ion spectra of the first 54 encounters, we observed that:

[28] A large part of the encounters can be assigned into the four basic classes (plasma sheet, lobe-like, magnetosheath and heavy-rich) according to their ion structure. Each different groups separated by using the ion data can be

Table 1. The Classification of the First 54 Encounters

Class	Ion Classification	Electron Classification[a]	Correspondence
		Basic Plasma Classes	
Lobe-like	T3, T4, T8, T10, T14, T18, T41	T3, T4, T8, T10, T14, T18, T41, T43	87%
Plasma sheet	TA, T5, T9, T11, T13, T15, T19, T23, T29, T33, T34, T36, T39, T44, T49, T51, T52, T53, T55	TA, T5, T9, T11, T13, T15, T19, T23, T29, T33, T34, T36, T39, T44, T49, T51, T52, T53, T55	100%
Heavy-rich/bimodal	T26, T31, T40, T46, T47	T26, T31, T40, T46, T47	100%
Magnetosheath	T32, T42	T32, T42	100%
		Other	
Mixed	TB, T6, T12, T20, T21, T24, T27, T28, T30, T35, T38, T43, T50, T54	TB, T6, T12, T20, T21, T22, T24, T28, T30, T50, T54	
Unclassified	T16, T17, T22, T25, T37, T45, T48	T16, T17, T25, T27, T35, T37, T38, T45, T48	

[a]*Rymer et al.* [2009].

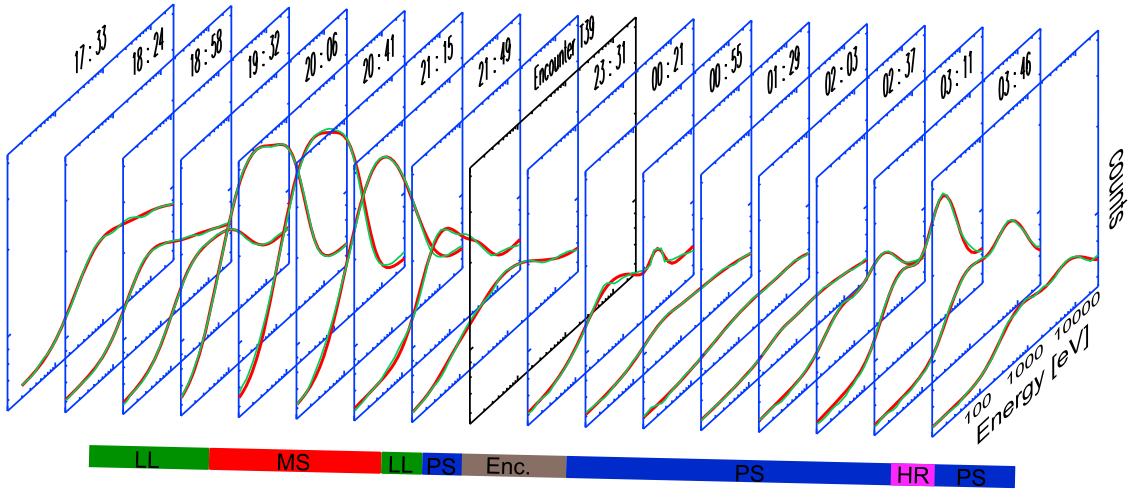

Figure 3. Energy spectra and automatic fits of 34 min long time intervals around encounter T39.

identified as one of the classes (plasma sheet, lobe-like, magnetosheath and bimodal respectively) of the electron classification. The ion classification of the encounters (at least according to the encounters which can be clearly classified into one of the basic plasma types) is almost in one to one correspondence with the electron classification; see Table 1. As for the "unclassified" and "mixed" classes, there are more differences, but these differences are mostly unphysical (due to e.g., data gaps, bad viewing or the limitations of one of the classification methods).

[29] Encounters categorized as "mixed" are combinations of shorter time intervals showing the characteristics of several clear types. In reality all encounters are somewhat mixed, few hour long upstream measurements cannot be characterized by a single type.

5. Statistical Studies

[30] We found that the most important type (appearing most frequently during our analysis) is the "mixed" type. In reality the few hour long upstream measurements are always mixed. They cannot be characterized by a single type; they are always a combination of shorter time intervals showing plasma properties of the four different clear classes. Clear classification is only possible for shorter time intervals; half an hour is short enough for most cases.

[31] Since the length of the SKR period is around 10 h, we need longer ±6 h window of interest around the encounters, to be able to study the SKR dependence as well.

[32] Bearing these two requirements in mind, we studied 2048 s (~34 min) long time intervals (always whole TOF cycles in accordance with the data acquisition characteristics of the CAPS instrument [*Young et al.*, 2004]) in a twelve hours long window of interest.

[33] There were ~12–17 intervals per window of interest around each encounter, so we studied some 700 intervals in all. We used a software tool to automatically classify these 700 intervals, the operation of which is based on the significant differences in the spectral properties of the various types. The magnetosheath, plasma sheet and lobe-like parts can be easily distinguished by using these spectral properties. The code fits a two-peaked function for the spectra with 7 parameters:

$$f(x) = A_0 + A_1 \exp\left(-A_3(x - A_2)^2\right) + A_4 \exp\left(-A_6(x - A_5)^2\right), \tag{1}$$

where x is the logarithm of the energy. The exact form of the test function is not essential. We have run the code with other test functions as well (e.g., using the combination of two Lorentzian peaks instead of the two Gaussians of equation (1)). Although equation (1) provides the best fit for most of the intervals, the difference is usually negligible. The important part is the parameter set, which try to reflect the physical properties of the two-peaked spectrum as much as possible. These parameters contain information about the background (A_0), the (absolute and relative) corotation energies of the two ion populations (A_2, A_5), their count rates (A_1, A_4) and thermal speeds (A_3, A_6).

[34] The actual code is an IDL program, which uses the CURVEFIT() function to fit equation (1). The initial guesses of the function's parameters were calculated from manually fine-tuned fits for the four typical example spectra of the four basic plasma types (T18, T23, T31, and T32 shown in Figure 2). The fit is performed for all four set of initial parameters, then again a fifth time, using the best result of the previous steps as initial parameter set. After stability and error checks, the best fit is saved.

[35] Figure 3 shows an example for the capabilities of the method; several energy spectra and automatic fits around encounter T39. Six of the seven parameters (A_1–A_6: the locations, heights, and widths of the two peaks) are significantly different for the four basic types; making it possible to classify the intervals using them.

[36] The magnetosheath type forms a distinct population in the parameter space, while the three other types can be characterized by well-defined but gradual variation of the parameters.

[37] Examining the 600+ processed intervals together, we found that the actual thermal speed (as measured by the width of the peak) of the heavy component is significantly

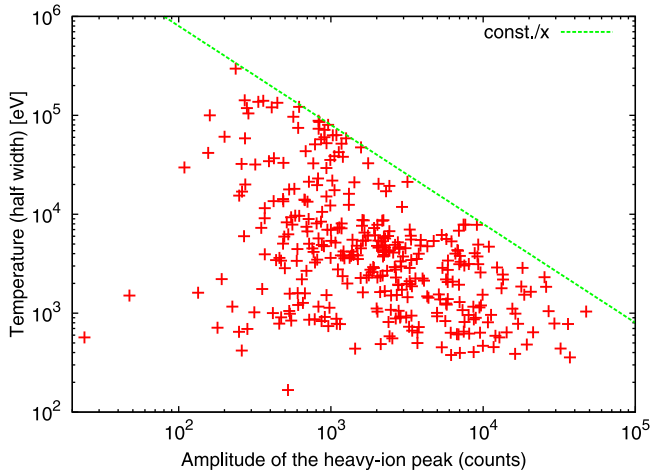

Figure 4. The temperature dependence of the heavy count rates. The higher count rates clearly coincide with the lower thermal speeds.

lower in the denser regions (Figure 4), which indicates lower temperatures in these regions. A more detailed discussion of these features will be presented in a follow-up paper.

[38] As we mentioned earlier, the bimodal type ion data is characterized by a high and narrow (dense and cold) heavy ion peak. Encounters classified as bimodals are dominated by this type of plasma; but we found short events with the spectral properties of this type far away from the bimodal encounters as well. We have not yet characterized the electron properties of these short events, so we will call them heavy-rich (HR) events instead of bimodal.

[39] In each 12 h long window of interest we found a clear structure in time as well as in SKR longitude: Almost every period of 12 h contain lobe-like, plasma sheet and heavy-rich intervals with a (few) short-time, heavy-rich "peak(s)" in the middle of a longer "slope" of plasma sheet type. All this structure is embedded in an even longer period of lobe-like plasma. Figure 5 shows an example (T17) of this time structure. Similar structures were found for almost every windows of interest, although it is common to have more then one heavy-rich peaks inside a plasma sheet region. Since the distance from Saturn is between 18 and 22 R_S (less then 20% variation) during these 12 h long periods, the radial variation of the ion density is much too small to explain these strong structures.

[40] The short heavy-rich events are characterized not only by their much higher heavy ion content, but their lower energy and thermal speed; they are short in time, localized in SKR longitude, and they are often in the middle of a longer "plasma sheet" period. The magnetic signatures of these events show that most of the HR events are associated with a special magnetic event; the most characteristic feature of which is that in KRTP (Kronian $\boldsymbol{r}\ \theta\ \varphi$ spherical coordinates) $B_{\boldsymbol{r}}$ sharply decreases inside these events. All these findings suggest that the magnetodisk plays an important role in the formation of the observed time/SKR structure.

5.1. The Role of the Magnetodisk

[41] The ion signatures as well as the magnetic signatures can be explained by identifying the heavy-rich events with magnetodisk crossings.

[42] The magnetic signatures can be understood by the following argument: When the spacecraft encounters the central sheet of the magnetodisk near the orbit of Titan, the magnetodisk is evidently close to the equatorial plane of Saturn. Thus in such a case that part of the magnetodisk is nearly parallel to the $\boldsymbol{r}$ direction of the KRTP coordinate system. This means that the $B_{\mathbf{r}}$ component is also parallel to the disk there. By definition the component of the magnetic field, which is parallel to the magnetodisk disappears in the central sheet itself. In our case, this component is $B_{\mathbf{r}}$, which (in a magnetodisk crossing) approaches zero, in accordance with the observed behavior.

[43] The ion signatures can also be explained by this picture. The sharp curvature of the field lines together with the rotation of the plasma generates a deep centrifugal potential well for the ions near the magnetodisk. The phenomenon of centrifugal separation can account for the observed properties of the heavy-rich events: In a centrifugal potential, the higher the mass of a particle, the more concentrated its spatial distribution. On the other hand the lower temperature part of the energy distribution of any ion species can be much more confined in a potential well than its higher temperature part (provided that the thermalization of the distribution is slow enough). Both the proton group and the heavy component are concentrated in the vicinity of the central sheet of the magnetodisk, but the heavy peak is more pronounced due to the higher mass.

[44] As the distance of the spacecraft and the magnetodisk increases the probe finds itself in warmer, more and more dilute plasma, at first in plasma sheet then lobe-like environments. Figure 5 shows how the amplitudes of the heavy and the light ion peaks change during a typical magnetodisk crossing. When the probe is inside the central sheet of the magnetodisk, the heavy ion count rate is more than four times higher than that of the light ions.

5.2. SKR Dependence

[45] One can learn from *Arridge et al.* [2008] and *Khurana et al.* [2009] that the magnetodisk has an asymmetric bowl-shaped structure, and this structure corotates with the Saturn Kilometric Radiation (SKR) based SLS3

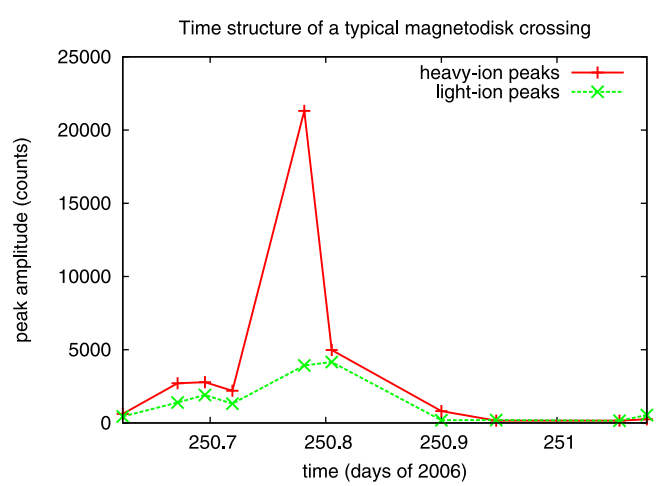

Figure 5. An example for the time structure: The amplitude of the heavy and light ion peaks in a 12 h long window of interest around encounter T17.

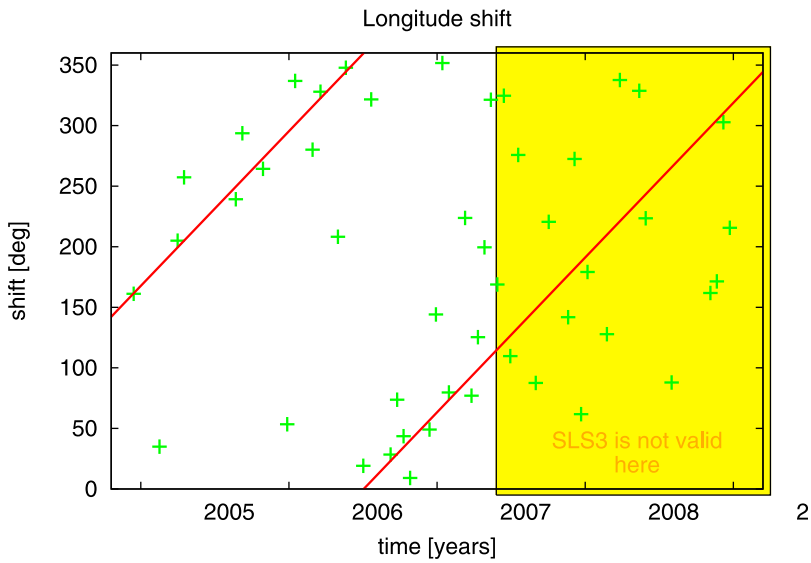

Figure 6. The phase shift needed to move the heavy-rich events to a given position in the SKR SLS3 coordinate system. Until the middle of 2007 the shift is roughly 0.35°/day (continuous line); after that day the SLS3 system is no longer valid.

longitude system. Provided that this model is appropriate the SKR longitude of the heavy-rich events should show a well-defined periodicity. Since the short intense peak in the heavy ion count rate is the most distinguishable feature of the heavy rich event and so, according to our hypothesis, of the magnetodisc crossing, the occurrences of these peaks should be well ordered in the SKR system.

[46] If we examine all the intervals together, at first sight we find no significant SKR structure. But for shorter time periods a periodicity reveals: there really is a long-term SKR dependence, but the phase of the peak slowly shifts away. This shift masks the consequences of the SKR periodicity if the statistical study covers a time period longer than a few months. To be able to study the SKR dependence, we have to compensate this slow shift.

[47] Figure 6 shows the phase shift needed to move the HR events to a given position in SKR. It can be seen that in the validity region of SKR SLS3 this shift is a mere 0.35 deg/day (0.04%) alteration of the periodicity. After the August of 2007 the SLS3 longitude system is no longer valid, furthermore in the first quarter of 2007 the second SKR period becomes significant [*Gurnett et al.*, 2009]. Thus we do not expect clear SLS3 dependence after the beginning of that year. In Figure 6 we can see that the shifts become disordered after April 2007, in accordance with the expectations. So we can state that the occurrence of the HR events is periodic; the periodicity is almost but not exactly the same as that of the SKR SLS3. The fourth version of the SKR based SLS is in preparation [*Gurnett et al.*, 2010]; we intend to analyze the periodicity with respect to the refined system later.

6. Conclusions

[48] Using CAPS ion measurements, we identified different plasma environment types of the Kronian magnetosphere in the vicinity of the first 54 Titan encounters and presented the characteristic features of the different environments.

[49] We found that the *Rymer et al.* [2009] classification of the Titan encounters is supported by the ion data; different classes have significantly different ion signatures. Mixed encounters are combinations of the clear types.

[50] Almost all few hour long data sets show mixed characteristics however. Shorter time intervals can be clearly classified based on the differences of their ion spectral properties.

[51] We studied more than 600 shorter intervals, which enabled us to perform statistical studies. Expanding the time interval to 12 h to cover full SKR periods, and taking into account the composition of the ions, we showed that the longer intervals include all the previous categories, and a special one, a short event, rich in heavy ions. We showed that such events occur at magnetodisk crossings.

[52] It was shown that the distance from the magnetodisk strongly influences the type of the upstream environment.

[53] The ion data reveals the fine structure of the magnetodisk, having a narrow central sheet of very high heavy ion content.

[54] The temperature of the heavy ions (as measured by the width of their energy distribution) is significantly lower in the central sheet of the magnetodisk.

[55] We also proved that the heavy rich events appear periodically in longitude, but with a period slightly (by 0.35°/day or 0.04%) longer than the SLS3 period.

[56] The ion signatures of the heavy rich events and bimodal encounters are very similar. It is probable that in the bimodal encounters the spacecraft remains near the central sheet of the magnetodisk for a longer time.

[57] **Acknowledgments.** The authors thank Michelle F. Thomsen for helpful discussion. The Hungarian authors acknowledge the financial support of the Hungarian Space Office.

[58] Robert Lysak thanks Alexander Lipatov and another reviewer for their assistance in evaluating this paper.

References

Arridge, C. S., K. K. Khurana, C. T. Russell, D. J. Southwood, N. Achilleos, M. K. Dougherty, A. J. Coates, and H. K. Leinweber (2008), Warping of Saturn's magnetospheric and magnetotail current sheets, *J. Geophys. Res.*, *113*, A08217, doi:10.1029/2007JA012963.

Backes, H., et al. (2005), Titan's magnetic field signature during the first Cassini encounter, *Science*, *308*(5724), 992–995, doi:10.1126/science.1109763.

Burch, J. L., A. D. DeJong, J. Goldstein, D. T. Young (2009), Periodicity in Saturn's magnetosphere: Plasma cam, *Geophys. Res. Lett.*, *36*, L14203, doi:10.1029/2009GL039043.

Galand, M., R. V. Yelle, A. J. Coates, H. Backes, J.-E. Wahlund (2006), Electron temperature of Titan's sunlit ionosphere, *Geophys. Res. Lett.*, *33*, L21101, doi:10.1029/2006GL027488.

Galopeau, P. H. M., and A. Lecacheux (2000), Variations of Saturn's radio rotation period measured at kilometer wavelengths, *J. Geophys. Res.*, *105*(A6), 13,089–13,102, doi:10.1029/1999JA005089.

Gombosi, T. I., T. P. Armstrong, C. S. Arridge, K. K. Khurana, S. M. Krimigis, N. Krupp, A. M. Persoon, and M. F. Thomsen (2009), Saturn's magnetospheric configuration, in *Saturn from Cassini-Huygens*, edited by M. Dougherty, L. Esposito, and T. Krimigis, chap. 9, pp. 203–255, Springer, Netherlands, doi:10.1007/978-1-4020-9217-6_9.

Gurnett, D. A., F. L. Scarf, and W. S. Kurth (1982), The structure of Titan's wake from plasma wave observations, *J. Geophys. Res.*, *87*, 1395–1403, doi:10.1029/JA087iA03p01395.

Gurnett, D. A., et al. (2005), Radio and plasma wave observations at Saturn from Cassini's approach and first orbit, *Science*, *307*(5713), 1255–1259, doi:10.1126/science.1105356.

Gurnett, D. A., A. Lecacheux, W. S. Kurth, A. M. Persoon, J. B. Groene, L. Lamy, P. Zarka, and J. F. Carbary (2009), Discovery of a north-south asymmetry in Saturn's radio rotation period, *Geophys. Res. Lett.*, *36*, L16102, doi:10.1029/2009GL039621.

Gurnett, D. A., J. B. Groene, A. M. Persoon, W. S. Kurth, M. G. Kivelson, K. K. Khurana, D. J. Southwood, and M. K. Dougherty (2010), Variations in the rotational modulation of Saturn kilometric radiation and their relationship to magnetic periodicities observed before and near equinox, Abstract SM31C-06 presented at 2010 Fall Meeting, AGU, San Francisco, Calif., 13–17 Dec.

Kellett, S., E. J. Bunce, A. J. Coates, S. W. H. Cowley (2009), Thickness of Saturn's ring current determined from north-south Cassini passes through the current layer, *J. Geophys. Res.*, *114*, A04209, doi:10.1029/2008JA013942.

Khurana, K. K., D. G. Mitchell, C. S. Arridge, M. K. Dougherty, C. T. Russell, C. Paranicas, N. Krupp, and A. J. Coates (2009), Sources of rotational signals in Saturn's magnetosphere, *J. Geophys. Res.*, *114*, A02211, doi:10.1029/2008JA013312.

Kurth, W. S., T. F. Averkamp, D. A. Gurnett, J. B. Groene, A. Lecacheux, A. (2008), An update to a Saturnian longitude system based on kilometric radio emissions, *J. Geophys. Res.*, *113*, A05222, doi:10.1029/2007JA012861.

Linder, D. R., A. J. Coates, R. D. Woodliffe, C. Alsop, A. D. Johnstone, M. Grande, A. Preece, B. Narheim, and D. T. Young (1998), The Cassini CAPS Electron Spectrometer, in *Measurement Techniques in Space Plasmas: Particles*, *Geophys. Monogr. Ser.*, vol. 102, edited by R. F. Pfaff, J. E. Borovsky, and D. T. Young, pp. 257–262, AGU, Washington, D. C.

McComas, D. J., J. E. Nordholt, J.-J. Berthelier, J.-M. Illiano, and D. T. Young (1998), The Cassini Ion Mass Spectrometer, in *Measurement Techniques in Space Plasmas: Particles*, *Geophys. Monogr. Ser.*, vol. 102, edited by R. F. Pfaff, J. E. Borovsky, and D. T. Young, pp. 187–194, AGU, Washington, D. C.

Nemeth, Z., K. Szego, L. Foldy, M. F. Thomsen, D. Delapp, A. J. Coates, A. Wellbrock, and Z. Bebesi (2010), The anatomy of two nightside magnetodisk crossings near Titan, Abstract SM11C-1759 presented at 2010 Fall Meeting, AGU, San Francisco, Calif., 13–17 Dec.

Ness, N. F., M. H. Acuna, and K. W. Behannon (1982), The induced magnetosphere of Titan, *J. Geophys. Res.*, *87*, 1369–1381, doi:10.1029/JA087iA03p01369.

Niemann, H. B., et al. (2005), The abundances of constituents of Titan's atmosphere from the GCMS instrument on the Huygens probe, *Nature*, *438*(7069), 779–784, doi:10.1038/nature04122.

Nordholt, J. E., J.-J. Berthelier, D. M. Burr, H. O. Funsten, R. Goldstein, J.-M. Illiano, K. P. McCabe, D. J. McComas, D. M. Potter, and D. T. Young (1998), The Cassini Ion Mass Spectrometer: Performance metrics and techniques, in *Measurement Techniques in Space Plasmas: Particles*, *Geophys. Monogr. Ser.*, vol. 102, edited by R. F. Pfaff, J. E. Borovsky, and D. T. Young, pp. 209–214, AGU, Washington, D. C.

Rymer, A. M., H. T. Smith, A. Wellbrock, A. J. Coates, and D. T. Young (2009), Discrete classification and electron energy spectra of Titan's varied magnetospheric environment, *Geophys. Res. Lett.*, *36*, L15109, doi:10.1029/2009GL039427.

Simon, S., F. M. Neubauer, C. L. Bertucci, H. Kriegel, J. Saur, C. T. Russell, and M. K. Dougherty (2010), Titan's highly dynamic magnetic environment: A systematic survey of Cassini magnetometer observations from flybys TA-T62, *Planet. Space Sci.*, *58*(10), 1230–1251, doi:10.1016/j.pss.2010.04.021.

Sittler, E. C., et al. (2009), Saturn's magnetosphere and properties of upstream flow at Titan: Preliminary results, paper presented at Magnetospheres of the Outer Planets 2009, Inst. of Geophys. and Meteorol., Univ. of Cologne, Cologne, Germany.

Southwood, D. (2011), Direct evidence of differences in magnetic rotation rate between Saturn's northern and southern polar regions, *J. Geophys. Res.*, *116*, A01201, doi:10.1029/2010JA016070.

Szego, K., Z. Nemeth, G. Erdos, L. Foldy, M. F. Thomsen, and D. Delapp (2010), The plasma environment of the magnetodisk of Saturn near Titan encounters as derived from ion densities measured by the Cassini/CAPS instrument, Abstract SM11C-1758 presented at 2010 Fall Meeting, AGU, San Francisco, Calif., 13–17 Dec.

Thomsen, M. F., and D.M. Delapp (2005), Numerical moments computation for CAPS/IMS, *Rep. LA-UR-05-1542*, Los Alamos Natl. Lab., Los Alamos, N. M.

Thomsen, M. F., D. B. Reisenfeld, D. M. Delapp, R. L. Tokar, D. T. Young, F. J. Crary, E. C. Sittler, M. A. McGraw, and J. D. Williams (2010), Survey of ion plasma parameters in Saturn's magnetosphere, *J. Geophys. Res.*, *115*, A10220, doi:10.1029/2010JA015267.

Vilppola, J. H., P. J. Tanskanen, B. L. Barraclough, and D. J. McComas (2001), Comparison between simulations and calibrations of a high resolution electrostatic analyzer, *Rev. Sci. Instrum.*, *72*(9), 3662–3669, doi:10.1063/1.1392337.

Wilson, R. J., R. L. Tokar, M. G. Henderson, T. W. Hill, M. F. Thomsen, and D. H. Pontius Jr. (2008), Cassini plasma spectrometer thermal ion measurements in Saturn's inner magnetosphere, *J. Geophys. Res.*, *113*, A12218, doi:10.1029/2008JA013486.

Young, D. T., et al. (2004), Cassini Plasma Spectrometer investigation, *Space Sci. Rev.*, *114*(1–4), 1–112, doi:10.1007/s11214-004-1406-4.

Z. Bebesi, Max Planck Institute for Solar System Research, Max Planck Str. 2, D-37191 Katlenburg-Lindau, Germany.

A. J. Coates and A. Wellbrock, Planetary Group, Mullard Space Science Laboratories, University College London, Holmbury St Mary, Dorking, Surrey RH5 6NT, UK.

G. Erdős, L. Foldy, Z. Németh, and K. Szego, Department of Space Physics, KFKI Research Institute for Particle and Nuclear Physics, PO Box 49, H-1225 Budapest, Hungary. (nemeth@rmki.kfki.hu)

A. Rymer, Johns Hopkins University Applied Physics Laboratory, 11100 Johns Hopkins Rd., Laurel, MD 20723, USA.

E. C. Sittler, NASA Goddard Space Flight Center, Greenbelt, MD 20771, USA.